PHYSICAL REVIEW A VOLUME 12, NUMBER 3 SEPTEMBER 1975

Density sensitive lines of highly ionized iron

G. A. Doschek and U. Feldman
E. O. Hulburt Center for Space Research, Naval Research Laboratory, Washington, D.C. 20375

J. Davis
Plasma Physics Branch, Naval Research Laboratory, Washington, D.C. 20375

R. D. Cowan
The University of California, Los Alamos Scientific Laboratory, Los Alamos, New Mexico 87544

(Received 21 November 1974; revised manuscript received 14 May 1975)

Spectral lines from ions in the nitrogen isoelectronic sequence due to transitions of the type, $2s2p^4\,{}^2D_{3/2,5/2}$-$2p^5\,{}^2P_{3/2}$, and $2s2p^4\,{}^2D_{3/2}$-$2p^5\,{}^2P_{1/2}$, are identified in the 100-Å region in laser-produced plasma spectra of titanium (Ti XVI) through cobalt (Co XXI). It is proposed that the intensities of these lines relative to the intensities of lines of the same ions due to transitions of the type $2s^22p^3$-$2s2p^4$ are sensitive to electron density in the range from $\approx 10^{18}$ to $\approx 10^{20}$ cm^{-3}. Calculations are performed for Fe XX, and a similar calculation is performed for a density-sensitive line ratio of Fe XIX, i.e., $(2s2p^5\,{}^1P_1$-$2p^6\,{}^1S_0)/(2s^22p^4\,{}^1S_0$-$2s2p^5\,{}^1P_1)$. This line ratio is also sensitive to electron density between about 10^{18} and 10^{20} cm^{-3}. The $2s2p^5\,{}^1P_1$-$2p^6\,{}^1S_0$ line is newly indentified in Cr XVII, Co XX, and Ni XXI.

I. INTRODUCTION

We have recently obtained x-ray and extreme-uv spectra of high temperature ($T_e \approx 10^6 - 10^7$ K) plasmas produced by the 100-GW glass laser system developed at the Naval Research Laboratory. We were particularly interested in identifying lines of highly ionized iron due to transitions of the type $2s^22p^k$–$2s2p^{k+1}$, because of their astrophysical importance. These lines fall near 100 Å and are emitted by iron lines from Fe XVIII through Fe XXIII. The iron lines are prominent in the spectra of solar flares.[1]

We were successful in identifying most of the strong lines emitted by ions of elements isoelectronic to Fe XVIII through Fe XXII.[2,3,4,5] The target elements ranged from titanium through nickel. Lines of ions isoelectronic to Fe XXIII have not yet been identified on laboratory plates. In some cases, the work on titanium and vanadium overlaps work done previously by Fawcett.[6]

Most of the identifications of the lines were made by extrapolating wavelengths of lines of lighter ions in the fluorine through boron isoelectronic sequences. A summary of the lighter ion data is given by Fawcett.[6] Classifying the lines was also facilitated through the use of theoretical wavelengths and oscillator strengths calculated by one of us (R. D. C.). The computer programs used to obtain the theoretical results are *ab initio* HX calculations that include intermediate coupling, configuration interaction, and relativistic corrections. Detailed descriptions of these programs are given by Cowan.[7,8] Another aid to classifying the lines was to compare spectra obtained with the focusing lens of the laser focused on the target, with spectra obtained with the focusing lens slightly off-focus. Lines of the highest ionization stages, e.g., Fe XXII, are weak or absent in the off-focus spectra, and therefore the lines of high ionization stages could be distinguished from lines of low degrees of ionization by visual inspection of the spectra. This technique is described in more detail and illustrated in Feldman *et al.*[4]

In this paper we report the identification of three additional lines in the nitrogen isoelectronic sequence (Fe XX) due to transitions of the type, $2s2p^4$ –$2p^5$. These lines are not intense in solar flare plasmas because of the low electron densities encountered ($N_e \sim 10^{11}$ cm^{-3}).[9] However, the lines are strong in spectra of laser-produced plasmas. We have found line intensity ratios involving these lines that are sensitive to electron density in the range from 10^{18} to about 10^{20} cm^{-3} in regions of the plasma where electron impact excitation rates are much larger than recombination rates. This range of electron densities is typical for the line-emitting regions of laser-produced plasmas.[10,11] The lines may therefore provide a good spectroscopic diagnostic method for measuring electron densities in some of these plasmas, and may also be applicable to high-density plasmas produced by sources other than lasers. Limitations on the use of the method are indicated below.

Fawcett *et al.*[12] have also published wavelengths for a similar density-sensitive line in the oxygen isoelectronic sequence for some of the elements from titanium through iron. This line is due to a transition of the type, $2s2p^5\,{}^1P_1 - 2p^6\,{}^1S_0$. We identified this line in spectra of chromium (Cr XVII), cobalt (Co XX), and nickel (Ni XXI). These new identifications, with some of our wavelengths for the other ions, are given in Table I.

II. EXPERIMENT

The laser system used to produce the high-temperature plasmas consisted of the mode-locked Nd:YAlG oscillator, a Pockel's cell gate which switched out a single pulse with an energy of a few millijoules, two Nd:YAlG preamplifiers, three Nd:glass amplifiers and a second Pockel's cell gate, which was used for isolation. The wavelength of the laser radiation was 1.06 μm. The pulse duration was controlled by Fabry-Perot étalons in the oscillator cavity to be 0.9 nsec. The energy on target ranged from ~3 J (3 GW) to as much as 60 J (60 GW). McMahon and Emmett[13] have described the early development of the laser system. A more recent description is given by McMahon and Barr.[14]

The laser beam was deflected by means of a prism through a 70-mm-diam 12-cm focal-length lens, which focused the beam onto the solid targets enclosed in vacuum. The resulting plasma, produced by conversion of laser energy into thermal energy of the target material, was on the order of 100 μm in diameter, for a well-focused beam, and had a lifetime of the order of nanoseconds. Radiation from the plasma passed through a 3-μm slit into a grazing incidence spectrograph.

The spectrograph used for the work described in this paper is a 3-m (88°) grazing-incidence instrument designed for a rocket-borne solar experiment. It is equipped with a 1200-line/mm Bausch and Lomb gold replica grating blazed at 2° 35′. The resolution is about 0.015 Å at 100 Å and is nearly constant throughout the spectral range covered. The spectra were recorded on Kodak 101 glass plates, and represent a time-averaged view of the plasma. A more detailed description of the spectrograph is given elsewhere.[15,16]

III. RESULTS

The identification of the Fe XX $2s2p^4\,{}^2D_{3/2,5/2}-2p^5\,{}^2P_{3/2}$ transitions and the Fe XX $2s2p^4\,{}^2D_{3/2}-2p^5\,{}^2P_{1/2}$ line was accomplished by determining the approximate wavelengths and relative intensities of the lines from the theoretical *ab initio* calculations discussed above. The pair of lines, $2s2p^4\,{}^2D_{3/2,5/2}-2p^5\,{}^2P_{3/2}$, was found by noting the presence of two lines near the theoretical wavelengths in iron spectra obtained from plasmas of different excitation conditions produced as discussed above. The relative intensities of these lines in the different spectra were typical of the relative intensities of identified Fe XX lines. The energy difference between the pair of iron lines, $^2D_{3/2}-{}^2P_{3/2}$, and $^2D_{5/2}-{}^2P_{3/2}$, turned out to be equal to within experimental error to the energy splitting between the $2s2p^4\,{}^2D_{3/2,5/2}$ levels as experimentally determined previously.[3] The $^2D_{3/2}-{}^2P_{1/2}$ Fe XX line was identified with the help of the *ab initio* calculations, and from extrapolations of wavelengths of these transitions recently identified by Fawcett and Hayes[17] in spectra of potassium through chromium. Only these three Fe XX lines due to $2s2p^4-2p^5$ transitions could be reliably identified in this manner. Most of the other possible nearby lines are either too weak, or fall in a wavelength region where the spectrograph is not efficient. After finding the lines in iron, it was easy to extrapolate to lighter ions and find the lines in spectra of manganese through titanium. One of the lines was found for cobalt and some of these lines were identified either previously or independently by Fawcett.[6,17] Table II lists the wavelengths and energies of the lines of the nitrogen isoelectronic sequence due to transitions $2s2p^4-2p^5$.

TABLE I. Transitions $2s2p^5\,{}^1P_1-2p^6\,{}^1S_0$ in the O I isoelectronic sequence.

Ion	λ (Å)	σ (cm^{-1})
Ti XV	147.45[a]	678 200
V XVI	138.17[a]	723 700
Cr XVII	129.75	770 700
Mn XVIII	122.25[a]	818 000
Fe XIX	115.40[a]	866 600
Co XX	109.14	916 300
Ni XXI	103.33	967 800

[a] Reported previously by Fawcett *et al*. (Ref. 12).

IV. DISCUSSION

In the following discussion, we confine our remarks to the regions of the plasma where electron impact excitation and radiative decay are primarily responsible for populating excited levels, and discuss the density sensitive lines that arise from $2p^{k+2}$ levels. Electron impact excitation is important in regions close to the target.[18] Line emission in regions far from the target, e.g., ≈ 1 mm, may be produced primarily by dielectronic and radiative recombination processes.[18] A more proper treatment of the problem would be to incorporate the atomic rate equations into a hydrodynamic model of the plasma.[19]

Because double-electron excitation has a much smaller cross section than single-electron excitation, the $2p^{k+2}$ levels are almost entirely populated by excitation from $2s2p^{k+1}$, rather than directly from $2s^22p^k$. Thus the $2s2p^{k+1}-2p^{k+2}$ lines become as intense as some of the $2s^22p^k-2s2p^{k+1}$ lines when the populations of the $2s^22p^k$ and

$2s2p^{k+1}$ levels become comparable. This occurs between the coronal regime of the ion, i.e., where radiative decay rates are much larger than collisional excitation and deexcitation rates, and the collisional regime, where radiative decay rates are much smaller than the collisional processes. In this intermediate regime, collisional rates are roughly comparable to radiative decay rates. This may be expressed as[20]

$$N_e C(2s^2 2p^k \rightarrow 2s2p^{k+1}) \approx A(2s2p^{k+1} \rightarrow 2s^2 2p^k) , \quad (1)$$

where N_e is the electron density, A is a spontaneous decay rate, and C is an electron impact excitation or deexcitation coefficient. Equation (1) is not an exact expression of detailed balance, but enables us to estimate the density regime where line ratios are density sensitive.

The excitation coefficient ($cm^3\ sec^{-1}$) is[20,21]

$$C^e_{ik} = \frac{2.7\times10^{-15} f_{ik} \langle \bar{g} \rangle_{ik} e^{-\Delta E_{ik}/kT_e}}{(T_e)^{1/2} \Delta E_{ik}} , \quad (2a)$$

and the deexcitation coefficient is

$$C^d_{ik} = (\omega_i/\omega_k)\, C^e_{ik}\, e^{\Delta E_{ik}/kT_e} , \quad (2b)$$

where f_{ik} is the absorption oscillator strength for the $i \rightarrow k$ transitions, T_e is the electron temperature in °K, ΔE_{ik} is the transition energy in ergs, and $\langle \bar{g} \rangle_{ik}$ is an effective Gaunt factor, and $\omega_i(\omega_k)$ is the statistical weight of the lower (upper) level. Because the temperatures of our laser-produced plasmas are $\approx 10^7$ K as determined from temperature-sensitive line ratios,[22] C_{ik} is only weakly dependent on the actual electron temperature, and the populations of the $2s2p^{k+1}$ levels, and hence the $2p^{k+2}$ levels, depend primarily on the electron density. From the *ab initio* wavelength and oscillator strength calculations for iron, a typical decay rate for a $2s^2 2p^k - 2s2p^{k+1}$ line is $A \sim 3\times10^{10}$ sec^{-1}, and from calculations of effective Gaunt factors performed by one of us (J. D.), $\langle \bar{g} \rangle_{ik} \approx 1$ for all transitions involved in iron. The Gaunt-factor calculations are described shortly. Combining either Eq. (2a) or (2b) with Eq. (1) gives $N_e \approx 10^{20}$ cm^{-3}, which is a typical density for line emitting regions of laser-produced plasmas.

We therefore decided to calculate the relative level populations for $2s2p^{k+1}$ and $2p^{k+2}$, so that the electron density could be determined more precisely from intensity ratios of the $2s2p^{k+1} - 2p^{k+2}$ lines to the $2s^2 2p^k - 2s2p^{k+1}$ lines. The calculations were done for Fe XIX and Fe XX, but could also be extended to other ions of the O I and N I sequence, and to other sequences such as the C I sequence, when line identifications become available. The specific processes included in the calculations were collisional excitation and deexcitation, and spontaneous radiative decay.

In order to calculate the relative level populations, values for the spontaneous decay rates and the effective Gaunt factors are needed. The decay rates are obtained from the theoretical calculations of Cowan discussed above. The effective Gaunt factors were obtained using the semiclassical impact theory for allowed transitions as developed by Alder *et al.*[23] and Seaton.[24] Seaton's formulation is modified as in Alder *et al.* in order to treat electron impact excitation of ions rather than neutrals. The connection between the effective Gaunt factor and the collision strength Ω_{ik} is[21]

$$\Omega_{ik} = (8\pi/3\sqrt{3})\, \omega_i\, R_{ik}\, \bar{g} , \quad (3)$$

and the collision strength is related to the cross section (cm^{-2}) by[24]

$$\sigma_{ik} = (I_H/E)\, (\Omega_{ik}/\omega_i)\, \pi a_0^2 . \quad (4)$$

In the above equations, ω_i is the statistical weight of the lower level i, R_{ik} is the square of the dipole matrix element in units of the Bohr radius, I_H is the hydrogen ionization potential, E is the incident electron energy, and a_0 is the Bohr radius in cm. $\bar{g} = \bar{g}(Z, E, \Delta E_{ik})$ is the dimensionless Gaunt factor obtained by solving the classical equations of motion. It is proportional to[21]

$$\bar{g} \propto e^{\pi\zeta}\, y K_{i\zeta}(y)\, |K'_{i\zeta}(y)| , \quad (5)$$

where K and K' are the modified Bessel function and its derivative, and $y = \zeta + \delta_0$ with

TABLE II. Lines of the N I isoelectronic sequence.

Ion	Classification	λ (Å)	σ (cm^{-1})
Ti XVI	$2s2p^4\,{}^2D_{5/2} - 2p^5\,{}^2P_{3/2}$	138.80[a,b]	720 500
	${}^2D_{3/2} - {}^2P_{3/2}$	138.02	724 500
	${}^2D_{3/2} - {}^2P_{1/2}$	129.07[b]	774 800
V XVII	$2s2p^4\,{}^2D_{5/2} - 2p^5\,{}^2P_{3/2}$	130.95[b]	763 600
	${}^2D_{3/2} - {}^2P_{3/2}$	129.94	769 600
	${}^2D_{3/2} - {}^2P_{1/2}$	120.30[b]	831 300
Cr XVIII	$2s2p^4\,{}^2D_{5/2} - 2p^5\,{}^2P_{3/2}$	123.83[c]	807 600
	${}^2D_{3/2} - {}^2P_{3/2}$	122.55	816 000
	${}^2D_{3/2} - {}^2P_{1/2}$	112.27[c]	890 700
Mn XIX	$2s2p^4\,{}^2D_{5/2} - 2p^5\,{}^2P_{3/2}$	117.43	851 600
	${}^2D_{3/2} - {}^2P_{3/2}$	115.84	863 300
	${}^2D_{3/2} - {}^2P_{1/2}$	104.89	953 400
Fe XX	$2s2p^4\,{}^2D_{5/2} - 2p^5\,{}^2P_{3/2}$	111.60	896 100
	${}^2D_{3/2} - {}^2P_{3/2}$	109.68	911 700
	${}^2D_{3/2} - {}^2P_{1/2}$	98.09	1 019 500
Co XXI	$2s2p^4\,{}^2D_{5/2} - 2p^5\,{}^2P_{3/2}$	106.23	941 400

[a] Blend with Ti XVI ($2s^2 2p^3\,{}^2P_{3/2} - 2s2p^4\,{}^2S_{1/2}$), Feldman *et al.* (Ref. 4).

[b] Previously identified by Fawcett or Fawcett, Galanti, and Peacock (Ref. 6, 12).

[c] Identified independently by Fawcett and Hayes (Ref. 17).

$$\zeta = \frac{Ze^2}{\hbar}\left|\frac{1}{V_i} - \frac{1}{V_f}\right| \tag{6}$$

and

$$\delta_0 = |V_i - V_f|\,(R_0\hbar/e^2)\ . \tag{7}$$

Here Z is the charge on the target (i.e., $Z \equiv 0$ for neutrals), $V_i(V_f)$ is the initial (final) electron velocity, e is the electronic charge, and R_0 (in atomic units) is given by

$$R_0 = [3n_{*l}^2 - l(l+1)]/2Z\ , \tag{8}$$

where n_{*l} is the effective principal quantum number of the state with orbital quantum number l.

The excitation rate ($\mathrm{cm^3\ sec^{-1}}$) is obtained by averaging over a Maxwellian velocity distribution, i.e.,

$$C_{ik} \equiv \langle v\sigma_{ik}\rangle = 16 I_H^2\,\pi a_0^2 \left(\frac{2\pi}{3mkT_e}\right)^{1/2} \frac{f_{ik}\langle\bar{g}\rangle_{ik}\, e^{-\Delta E_{ik}/kT_e}}{\Delta E_{ik}}\ , \tag{9}$$

where m is the electron mass and $\langle\bar{g}\rangle_{ik}$ is defined as[21]

$$\langle\bar{g}\rangle_{ik} = \int_{\Delta E_{ik}}^{\infty} \bar{g}\, e^{-E/kT_e}\,dE \Big/ \int_{\Delta E_{ik}}^{\infty} e^{-E/kT_e}\,dE\ , \tag{10}$$

and we have related R_{ik} to the oscillator strength f_{ik} by using the relation

$$f_{ik} = (\Delta E_{ik}/3I_H)\,R_{ik}\ . \tag{11}$$

Evaluation of the constants in Eq. (9) using cgs units leads to Eq. (2). From the development of Eq. (2) it is seen that Eq. (2) can be used to compute excitation rates for the $2s2p^{k+1}$–$2p^{k+2}$ transitions (i.e., transitions between two excited states) as well as for the $2s^22p^k$–$2s2p^{k+1}$ transitions.

In the O I sequence, the significant intensity ratios may be calculated very simply. There is only one strong line originating from the doubly excited level, i.e., $2s2p^5\,{}^1P_1$–$2p^6\,{}^1S_0$. The decay from $2p^6\,{}^1S_0$ to the other levels of the $2s2p^5$ configuration is negligible compared to the decay to $2s2p^5\,{}^1P_1$. If it is assumed that the $2p^6\,{}^1S_0$ level is populated primarily by electron impact excitation from the $2s2p^5\,{}^1P_1$ level, and depopulated by collision deexcitation and spontaneous decay to $2s2p^5\,{}^1P_1$, the following two equations can be written for calculating the ratio of intensities of the lines $2s2p^5\,{}^1P_1$–$2p^6\,{}^1S_0$, and $2s^22p^{4\,2S+1}L_J$–$2s2p^5\,{}^1P_1$:

$$N({}^1S_0)\,[A({}^1S_0 \to {}^1P_1) + N_e C^d({}^1S_0 \to {}^1P_1)] = N_e N({}^1P_1)\,C^e({}^1P_1 \to {}^1S_0)\ ,$$

$$\frac{I({}^1S_0 \to {}^1P_1)}{I({}^1P_1 \to {}^{2S+1}L_J)} = \frac{N({}^1S_0)}{N({}^1P_1)}\,\frac{A({}^1S_0 \to {}^1P_1)}{A({}^1P_1 \to {}^{2S+1}L_J)}\ , \tag{12}$$

where $N(j)$ is the population ($\mathrm{cm^{-3}}$) of the jth level; C^e and C^d are the collisional excitation and deexcitation coefficients, respectively; A is the spontaneous decay rate; and S, L, and J are the total spin, orbital, and total angular momentum of the level of the $2s^22p^k$ configuration.

For the N I sequence (Fe XX) it is more appropriate to derive the relative populations of all of the $2s^22p^k$, $2s2p^{k+1}$, and $2p^{k+2}$ levels, because there are several possible density sensitive lines. We have done this for Fe XX, and also for Fe XIX. Only electron-impact excitation and deexcitation, and radiative decay, were considered. Recombinations and excitation followed by cascade were neglected because the rates for these processes are small compared to electron impact excitation in the regions of the plasma that we are discussing.

In making these calculations, electron impact excitation and possible iron-ion impact-excitations from one level of a configuration to other levels of the same configuration are neglected. The maximum effect that these excitations can have on the derived electron densities can be determined by assuming that these processes are sufficiently large such that all the levels of each configuration are populated according to their statistical weights, and then solving for the relative populations of the $2s^22p^k$, $2s2p^{k+1}$, and $2p^{k+2}$ configurations as a function of electron density. The two calculations yield nearly identical results. The maximum difference in derived densities using the Fe XX line ratios discussed below is only a factor of 1.5. The densities are higher assuming statistical populations of the levels. Of course, the nondipole excitations have no effect on the Fe XIX density sensitive line ratio as can be seen from Eqs. (12). In this case, the density sensitive intensity ratio only depends on the assumption that the $2p^6\,{}^1S_0$ level is populated by electron impact from $2s2p^5\,{}^1P_1$.

The populations of the various levels are determined by solving the coupled equations

$$N_i\left[N_e\left(\sum_{k>i} C_{ik}^e + \sum_{k<i} C_{ik}^d\right) + \sum_{k<i} A_{ik}\right] = N_e\left(\sum_{k<i} N_k C_{ki}^e + \sum_{k>i} N_k C_{ki}^d\right) + \sum_{k>i} N_k A_{ki}\ , \tag{13}$$

where N_i is the population ($\mathrm{cm^{-3}}$) of the ith level, C_{ik}^e and C_{ik}^d are collisional excitation and deexcitation coefficients, respectively, and A_{ik} are the spontaneous decay rates. The intensity (photons $\mathrm{sec^{-1}\ sr^{-1}}$) of a line connecting the levels i and k is

$$I(i \to k) = (1/4\pi) N_i A_{ik} V , \quad (14)$$

where V is the plasma volume over which emission occurs.

Some of the results for Fe XIX and Fe XX are shown in Fig. 1. The electron temperature is assumed to be 9×10^6 K. Corrections to the electron densities for other temperatures can be estimated from Eq. (2). For example, if $T_e = 4.5\times10^6$ K, N_e should be reduced by about 20%.

The results shown in Fig. 1 are plotted as ratios of the line intensities indicated in the figure. The lines of Fe XIX at 106.12, 109.97, and 111.70 Å, and the 108.81 Å line of Fe XX, have been previously identified. With the exception of the fifth curve in Fig. 1, the curves will actually flatten out in the limit of low density instead of falling to zero. This is because there will be a very small contribution due to direct excitation from the $2s^22p^k$ levels into the $2p^{k+2}$ levels. A more refined treatment should consider this effect. The fifth curve in Fig. 1 gives the intensity ratio of the lines at 109.97 and 111.70 Å, both of which arise from the $2s2p^5\,{}^3P_1$ level of Fe XIX. Their intensity ratio is therefore independent of electron density and depends only on the spontaneous decay rates to the $2s^22p^4\,{}^3P_0$ and $2s^22p^4\,{}^3P_1$ levels (see Table III).

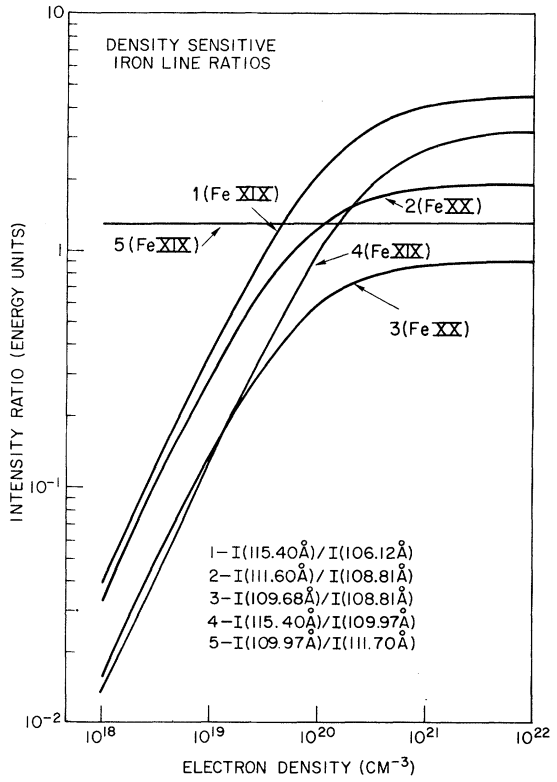

FIG. 1. Density sensitive line ratios of Fe XIX and Fe XX.

The iron lines at 115.40, 111.60, and 109.68 Å are good density indicators in the range from $N_e \simeq 10^{18}$ to $\simeq 10^{20}$ cm^{-3}, in regions of the plasma where electron impact excitation is the dominant excitation mechanism. Similar conclusions follow for other ions of the O I and N I isoelectronic sequences. We note that the above calculations should be incorporated into a non-steady-state model if it is determined that for a particular plasma, variations in plasma conditions occur over time scales on the order of 0.1 nsec, because 0.1 nsec is of the order of the lifetimes of the excited states of the iron ions.

Figure 2 shows a portion of an iron line spectrum obtained by us from a laser-produced plasma. A print of the complete spectrum between 90 and 118 Å is published in Feldman *et al.*[4] under the heading, "at focus." To obtain this spectrum, the spectrograph viewed most of the plasma, and therefore the spectrum is a time- and space-averaged representation of the plasma. The iron lines shown in Fig. 2 are summarized in Table III, and the identifications for the strong lines of the F I – B I isoelectronic sequences due to $2s^22p^k - 2s2p^{k+1}$ transitions are given elsewhere.[2-5] The trace of the spectrum shown in the lower part of the figure was made with a Grant microdensitometer.

The primary purpose in obtaining the spectrum shown in Fig. 2 was the identification and class-

TABLE III. Iron lines in laser-produced plasma spectrum.

Ion	Classification	λ (Å)	gf [f]
Fe XIX [a]	$2s^22p^4\,{}^1S_0 - 2s2p^5\,{}^1P_1$	106.12	0.056
Fe XIX [a]	$2s^22p^4\,{}^3P_1 - 2s2p^5\,{}^3P_0$	106.33	0.099
Fe XIX [a]	$2s^22p^4\,{}^3P_2 - 2s2p^5\,{}^3P_2$	108.37	0.32
Fe XIX [a]	$2s^22p^4\,{}^3P_0 - 2s2p^5\,{}^3P_1$	109.97	0.083
Fe XIX [a]	$2s^22p^4\,{}^3P_1 - 2s2p^5\,{}^3P_1$	111.70	0.067
Fe XIX [b]	$2s2p^5\,{}^1P_1 - 2p^6\,{}^1S_0$	115.40	0.32
Fe XX [c]	$2s^22p^3\,{}^2P_{1/2} - 2s2p^4\,{}^2S_{1/2}$	106.97	0.13
Fe XX [a]	$2s^22p^3\,{}^2P_{3/2} - 2s2p^4\,{}^2P_{3/2}$	108.81	0.12
Fe XX [d]	$2s2p^4\,{}^2D_{3/2} - 2p^5\,{}^2P_{3/2}$	109.68	0.12
Fe XX [a]	$2s^22p^3\,{}^2D_{3/2} - 2s2p^4\,{}^2D_{3/2}$	110.64	0.33
Fe XX [d]	$2s2p^4\,{}^2D_{5/2} - 2p^5\,{}^2P_{3/2}$	111.60	0.27
Fe XX [a]	$2s^22p^3\,{}^2D_{5/2} - 2s2p^4\,{}^2D_{5/2}$	113.36	0.36
Fe XX [c]	$2s^22p^2\,{}^1D_2 - 2s2p^3\,{}^1D_2$	113.31	0.59
Fe XXII [e]	$2s^22p\ {}^2P_{3/2} - 2s2p\ {}^2P_{3/2}$	114.39	0.51

[a] Feldman *et al.* and Doschek *et al.* (Refs. 2, 3).
[b] Fawcett *et al.* (Ref. 12).
[c] Feldman *et al.* (Ref. 4).
[d] Present paper.
[e] Doschek *et al.* (Ref. 5).
[f] Oscillator strength multiplied by the statistical weight of the lower level.

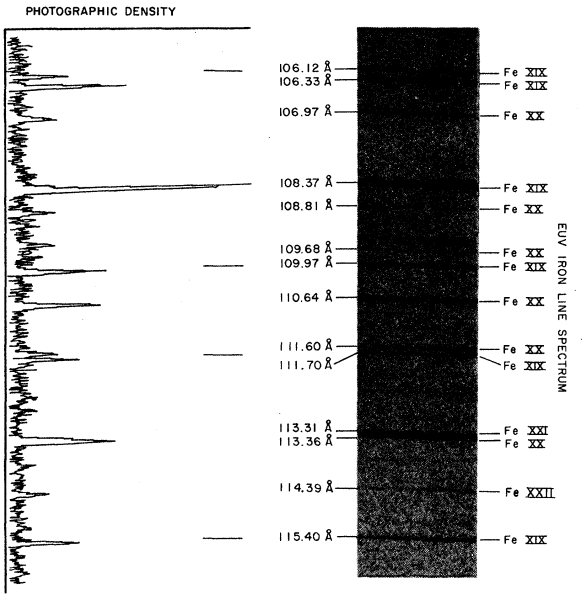

FIG. 2. Iron line spectrum and densitometer trace of a laser-produced plasma. The density-sensitive lines fall at 115.40, 111.60, and 109.68 Å. Complete identifications are given in Table III.

ification of lines of highly ionized iron. The experiment was not designed for accurate intensity measurements over substantial wavelength ranges. In particular, the grating efficiency decreases towards long wavelengths in an approximately linear fashion over the wavelength range in which most of iron lines fall (90–116 Å). The decrease in grating efficiency between $\simeq 98$ and $\simeq 112$ Å is about a factor of 2.

The shape of the response curve of the film can be inferred approximately from the grating efficiency and from the three Fe XIX lines at 101.56 Å (not shown in Fig. 2; see the photograph in Feldman *et al.*[4]), 109.97, and 111.70 Å. These three lines all arise from the $2s2p^5\,{}^3P_1$ level, and their intensity ratios are therefore known from the spontaneous decay rates. Using the response curve, the relative intensities of the lines in Fig. 2 can then be obtained from the photographic densities shown in the densitometer trace. The intensities derived in this manner of the Fe XIX and Fe XX lines that are not sensitive to electron density are in good agreement ($\approx 20\%$) with the predictions of Eqs. (13) and (14).

The time- and space-averaged electron density of the plasma can be found from the response curve and the density sensitive line ratios shown in Fig. 1, assuming that the steady-state treatment is applicable. Using Fig. 1, the intensity of the Fe XIX line at 115.4 Å, compared to the intensities of the 106.12, and 109.97, and 111.70 Å lines, gives an electron density of 2×10^{20} cm^{-3}. At an electron density of 2×10^{20} cm^{-3}, the density sensitive Fe XX lines are no longer very useful as density sensitive indicators (see Fig. 1). These lines are quite weak in our spectrum, and therefore the relative intensities are less reliable than the relative intensities of the Fe XIX lines. However, the ratios of the density sensitive 109.68 and 111.60 Å lines to the 108.81 Å line are consistent with a density above 10^{20} cm^{-3}, i.e., the photographic densities of the close pair of lines at 109.68 and 108.81 Å appear to be equal in the densitometer trace shown in Fig. 2, and the 111.60 Å line is noticably stronger than the 108.81 Å line. The measurement of electron density using the line ratio technique is not very reliable for the spectrum shown in Fig. 2 because the electron density indicated by the density sensitive lines is above 10^{20} cm^{-3}, where the line ratios in Fig. 1 flatten out and become less sensitive to density.

It is hoped that the line-ratio technique described in this paper can be successfully applied to calculate electron densities in plasmas where spatial and perhaps time resolution is obtainable. It may be possible in some cases to compare the electron densities derived from the line ratios with densities derived by independent means, such as by Thomson-scattered laser light or Stark broadening.

We thank Dr. R. C. Elton for reading the manuscript and offering helpful suggestions.

[1]S. O. Kastner, W. M. Neupert, and M. Swartz, Astrophys. J. 191, 261 (1974).
[2]U. Feldman, G. A. Doschek, D. J. Nagel, W. E. Behring, and Leonard Cohen, Astrophys. J. Lett. 183, L43 (1973).
[3]G. A. Doschek, U. Feldman, R. D. Cowan, and Leonard Cohen, Astrophys. J. 188, 417 (1974).
[4]U. Feldman, G. A. Doschek, R. D. Cowan, and Leonard Cohen, Astrophys. J. 196, 613 (1975).
[5]G. A. Doschek, U. Feldman, and Leonard Cohen, J. Opt. Soc. Am. 65, 463 (1975).
[6]B. C. Fawcett, S. R. C. Astrophysics Research Unit, Culham Laboratory, England, 1971 (special publication).
[7]R. D. Cowan, Phys. Rev. 163, 54 (1967).
[8]R. D. Cowan, J. Opt. Soc. Am. 58, 808 (1968).
[9]R. D. Cowan and K. G. Widing, Astrophys. J. 180, 285 (1973).

[10]U. Feldman, G. A. Doschek, D. J. Nagel, W. E. Behring, and R. D. Cowan, Astrophys. J. 187, 417 (1974).
[11]A. M. Malvezzi, E. Jannitti and G. Tondello (unpublished).
[12]B. C. Fawcett, M. Galanti, and N. J. Peacock, J. Phys. B. 7, 1149 (1974).
[13]J. M. McMahon and J. L. Emmett, *Record of the Eleventh Symposium on Electron, Ion, and Laser Beam Technology,* edited by R. F. M. Thornley (San Francisco Press, San Francisco, 1971).
[14]J. M. McMahon and O. C. Barr, *Proceedings of the Seventeenth Annual Meeting of the Society of Photo-Optical Instrumentation and Engineers, San Diego,* (S.P.I.E., Palos Verdes Estates, 1973), Vol. 41.
[15]W. E. Behring, R. J. Ugiansky, and U. Feldman, Appl. Opt. 12, 528 (1973).
[16]W. E. Behring, Leonard Cohen, and U. Feldman, Astrophys. J. 175, 493 (1972).
[17]B. C. Fawcett and R. W. Hayes, Mon. Not. R. Astron. Soc. 170, 185 (1975).
[18]K. G. Whitney and J. Davis, Appl. Phys. Lett. 24, 509 (1974).
[19]D. G. Colombant, K. G. Whitney, N. K. Winsor, J. Davis, and D. Tidman, Phys. Fluids (to be published).
[20]H. Van Regemorter, Astrophys. J. 136, 906 (1962).
[21]J. Davis, J. Quant. Spectrosc. Radiat. Transfer 14, 549 (1974).
[22]D. J. Nagel, P. G. Burkhalter, C. M. Dozier, J. F. Holzrichter, B. M. Klein, J. M. McMahon, J. A. Stamper, and R. R. Whitlock, Phys. Rev. Lett. 33, 743 (1974).
[23]K. Alder, A. Bohr, T. Huus, B. Mottelson, and A. Winther, Rev. Mod. Phys. 28, 432 (1956).
[24]M. J. Seaton, Proc. Phys. Soc. Lond. 79, 1105 (1962).

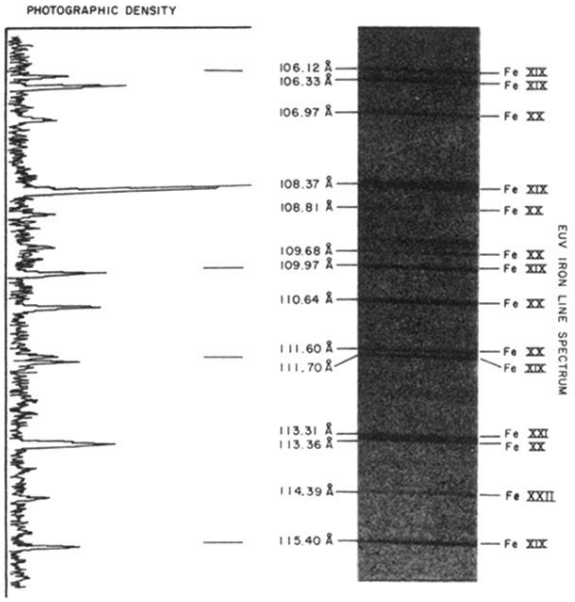

FIG. 2. Iron line spectrum and densitometer trace of a laser-produced plasma. The density-sensitive lines fall at 115.40, 111.60, and 109.68 Å. Complete identifications are given in Table III.